Rotational and Conformational Dynamics of *Escherichia coli* Ribosomal Protein L7/L12†

Brian D. Hamman,‡,§ Andrew V. Oleinikov,|| George G. Jokhadze,||,⊥ Robert R. Traut,|| and David M. Jameson*,‡

Department of Biochemistry and Biophysics, University of Hawaii, 1960 East-West Road, Honolulu, Hawaii 96822, and Department of Biological Chemistry, School of Medicine, University of California, Davis, California 95616

Received June 21, 1996; Revised Manuscript Received September 21, 1996⊗

ABSTRACT: Fluorescence methods were utilized to study dynamic aspects of the 24 kDa dimeric *Escherichia coli* ribosomal protein L7/L12. Oligonucleotide site-directed mutagenesis was used to introduce cysteine residues at specific locations along the peptide chain, in both the C-terminal and N-terminal domains, and various sulfhydryl reactive fluorescence probes ((iodoacetamido)fluorescein, IAEDANS, pyrenemethyl iodoacetate) were attached to these residues. In addition to the full-length proteins, a hinge-deleted variant and variants corresponding to the C-terminal fragment and the N-terminal fragment were also studied. Both steady-state and time-resolved fluorescence measurements were carried out, and the results demonstrated that L7/L12 is not a rigid molecule. Specifically, the two C-terminal domains move freely with respect to one another and with respect to the dimeric N-terminal domain. Removal of the hinge region, however, significantly reduces the mobility of the C-terminal domains. The data also show that the rotational relaxation time monitored by the fluorescent probe depends upon the probe's excited state lifetime. This observation is interpreted to indicate that a hierarchy of motions exists in the L7/L12 molecule including facile motions of the C-terminal domains and dimeric N-terminal domain, in addition to the overall tumbling of the protein. Probes attached to the N-terminal domain exhibit global rotational relaxation times consistent with the molecular mass of the dimeric N-terminal fragment. Upon reconstitution of labeled L7/L12 with ribosomal cores, however, the motion associated with the dimeric N-terminal domain is greatly diminished while the facile motion of the C-terminal domains is almost unchanged.

The proteins L7 and L12 are found in the large subunit of *Escherichia coli* ribosomes and are conserved among a diverse array of organisms (Möller et al., 1970; Matheson et al., 1980; Liljas, 1991). L7 differs from L12 in that the former is acetylated at its N-terminus (Terhorst et al., 1972). L7/L12[1] is the only ribosomal protein which occurs in multiple copies—it is present as four copies (two dimers) in the 50S ribosomal subunit. At least one dimer constitutes the conspicuous morphological feature known as the L7/L12 stalk. L7/L12 can be selectively removed from and reconstituted back into the ribosome with concomitant loss and recovery of activity (Hamel et al., 1972; Tokimatsu et al., 1981). The amino acid sequence of *E. coli* L7/L12 revealed that each monomer possesses 120 residues with a molecular weight of 12.2 kDa (Terhorst et al., 1972). L7/L12 is considered to be comprised of two distinct, organized, structural domains: a helical N-terminal domain (Möller & Maassen, 1986; Tsurugi & Mitsui, 1991; Bocharov et al., 1996), residues 1−36, responsible for dimer formation (Gudkov & Behlke, 1978; Gudkov et al., 1995) and for binding of the L7/L12 dimer to L10 in the 50S ribosomal subunit, and a globular C-terminal domain (Leijonmarck & Liljas, 1987), residues 53−120, responsible for interaction with factors (Van Agthaven et al., 1975; Sommer et al., 1985). These domains are separated by a putatively disordered "hinge" region, residues 35−52 (Gudkov et al., 1982; Cowgill et al., 1984; Leijonmarck & Liljas, 1987; Bushuev et al., 1989).

L7/L12 was initially characterized as a rigid, highly elongated dimer based on low-angle X-ray scattering, sedimentation velocity, and viscosimetry experiments (Österberg et al., 1976; Wong & Paradies, 1974; Luer & Wong, 1979, 1980); these studies reported axial ratios in the range of 8:1 to 19:1. More recently, neutron scattering studies reported an axial ratio of 6.5:1 for L7/L12 associated with the 50S ribosomal subunit (Nowotny et al., 1994). An elongated structure is also implied by cross-linking experiments which demonstrate that L7/L12 can cross-link to regions in the peptidyl transferase center known from neutron scattering studies to be around 100 Å distant from the L7/L12 stalk (Traut et al., 1986) and also to proteins in the 30S subunit (Traut et al., 1995). Cross-linking studies indicated that the so-called "hinge" region of L7/L12 facilitates the considerable mobility of the C-terminal domain (Zecherle et al., 1992a,b; Oleinikov et al., 1993b; Traut et al., 1993).

† This work was supported in part by NSF Grants DMB 9005195 and MCB 9506845 (D.M.J.) and NIH Grant GM 17924 (R.R.T.).

* To whom correspondence should be addressed.

‡ University of Hawaii.

§ Present address: Department of Medical Biochemistry and Genetics, Texas A&M University, 116 Reynolds Medical Building, College Station, TX 77843-1114.

|| University of California, Davis.

⊥ Present address: Clontech Laboratories Inc., 1020 East Meadow Circle, Palo Alto, CA 94303-4230.

⊗ Abstract published in *Advance ACS Abstracts,* November 15, 1996.

[1] Abbreviations: L7/L12 refers to an unfractionated mixture of L7 and L12; FITC, fluorescein isothiocyanate; 5-IAF, 5-(iodoacetamido)-fluorescein; 1,5-IAEDANS, 5-[[2-[(iodoacetyl)amino]ethyl]amino]-naphthalene-1-sulfonate; 1-PMIA, 1-pyrenemethyl iodoacetate; 5-AF, 1,5-AEDANS, and 1-PMA refer to the probes after reaction with the protein and loss of iodide; SE-HPLC, size-exclusion high-performance liquid chromatography; CTF, C-terminal fragment, residues 52−120, of L7/L12; NTF, N-terminal fragment, residues 1−53, of L7/L12; DMF, dimethylformamide; DTT, dithiothreitol.

S0006-2960(96)01500-0 CCC: $12.00

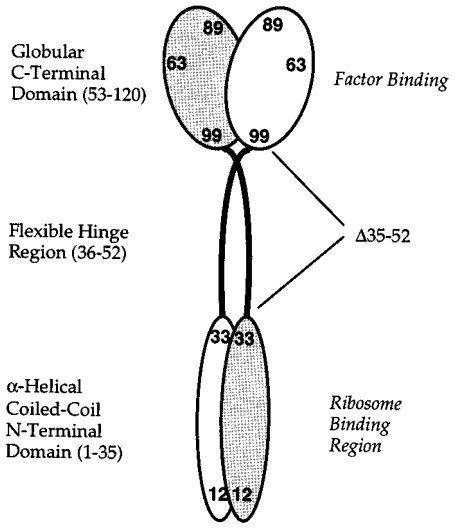

FIGURE 1: Schematic diagram of the domain structure of *E. coli* L7/L12 dimer indicating the sites of the various cysteine substitutions and the hinge deletion; this Figure is not meant to depict the solution conformation of L7/L12.

Mutants of L7/L12 lacking this hinge region are no longer competent to promote ribosome activity (Kirsebom et al., 1986; Gudkov et al., 1991; Traut et al., 1993; Oleinikov et al., 1993a). Flexibility of L7/L12 has also been inferred from proton NMR (Cowgill et al., 1984; Bushuev et al., 1984, 1989), ESR (Tritton, 1978), and electron microscopy (Verschoor et al., 1986). These studies suggest that L7/L12 does not behave as a rigid rod but rather can display flexibility and relative motion between the C- and N-terminal domains. In the present study, we investigated the motional properties of L7/L12 in more detail. To this end, fluorescent probes of varying lifetimes were attached to specific sites in L7/L12 which had cysteine residues introduced at different locations along the peptide chain (wild-type L7/L12 does not contain cysteine). A "hinge-deleted" variant of L7/L12, which lacks residues 42−52, was also investigated as were deletion variants corresponding to the C-terminal fragment (CTF; residues 52−120) and N-terminal fragment (NTF; residues 1−53). The motional properties of the C- and N-terminal domains of L7/L12 reconstituted with 70S ribosomal cores were also examined.

MATERIALS AND METHODS

Construction, Expression, and Purification of Recombinant L7/L12. Genetic constructions for Ser89→Cys89 and Ala63→Cys63 substitutions have been described (Zecherle et al., 1992a; Oleinikov et al., 1993a) as were the genetic constructions for Ser33→Cys33 substitution and Δ42−52 hinge deletion (Oleinikov et al., 1993b). Genetic constructions for Ala12→Cys12, NTF, and CTF were as previously described (Oleinikov et al., 1993a). In all cases, the DNA sequence was verified using the Sequenase T7 system from United States Biochemicals (Cleveland, OH). All procedures for overexpression, purification, and analysis of the protein variants have been described (Oleinikov et al., 1993a). The location of each of the substitutions and deletions is given in Figure 1. The full-length variants are designated C-12, C-33, C-63, and C-89; the double variants are designated C-89:Δ42−52 and C-89 CTF. The L7/L12 variants were always greater than 95% pure as judged by SDS−PAGE and laser scanning of the Coomassie Blue stained protein. To ensure stability of the methionines essential for dimerization of L7/L12 (Caldwell et al., 1978; Gudkov et al., 1978), proteins were stored between −20 and −100 °C in the presence of 7−15 mM β-mercaptoethanol or 4 mM DTT. Monomers of L7/L12 were formed from methionine oxidation as previously described (Caldwell et al., 1978; Gudkov et al., 1978), and purification of oxidized monomers was accomplished by gel filtration HPLC.

Probes and Labeling Protocols. All fluorescence probes were purchased from Molecular Probes, Inc. (Junction City, OR), and used without further purification. The protein labeling protocol was a modification of the method described by Allen (Allen, 1981; Hamman et al., 1996a). Specifically, labeling with the haloacetyl derivatives 5-IAF or 1,5-IAEDANS was carried out as follows: (1) 1−3 mg/mL protein was incubated with 1% β-mercaptoethanol for 30−60 min at 37, (2) the sample buffer was exchanged (using Biospin-6 filtration) with TMND buffer, pH 8.0, containing 50 mM Tris-HCl, 10 mM $MgCl_2$, 100 mM NH_4Cl, and 2−4 mM DTT, and 3) the fluorescent probe (dissolved in DMF) was then introduced to a final concentration of 8−10 mM and the solution was incubated at 37 °C for 40−75 min. Unreacted probe was removed by three Biospin-6 filtrations (equilibrated with TMND buffer, pH 7.4) or one Biospin-6 filtration followed by SE-HPLC. Under these conditions, wild-type L7/L12 did not react with haloacetyl probes. The dimeric aggregation state of the labeled L7/L12 was always verified by SE-HPLC prior to fluorescence measurements. Labeled full-length L7/L12 retained full activity in polyphenylalanine synthesis carried out as previously described (Zecherle et al., 1992b; Hamman et al., 1996a). Labeling of NTF, which did not contain cysteine residues, with FITC was carried out using the method described by Lee et al. (1981).

Labeling of the various L7/L12 cysteine mutants with 1-PMIA presented some difficulty due to probe precipitation in the labeling buffer. In the case of the C-33 variant, the labeling procedure described above led to good recovery of dimeric L7/L12 (judged by SE-HPLC). Conversely, labeling of the C-89 variant, the C-89:Δ42−52 variant, and, to a lesser extent, the C-63 variant with 1-PMIA resulted in protein aggregation as judged by SE-HPLC. The pyrene modified C-89 variant was not studied further, and dimeric pyrene modified C-63 variant was isolated by repetitive SE-HPLC to completely remove aggregates.

Quantification of Proteins and Probes. The extinction coefficients utilized for probes bound to L7/L12 were 70 000 M^{-1} cm^{-1} (5-AF; 488 nm), 5500 M^{-1} cm^{-1} (1,5-AEDANS; 351 nm), and 34 000 M^{-1} cm^{-1} (1-PMA; 351 nm). The extinction coefficient utilized for FITC bound to the NTF was 71 000 M^{-1} cm^{-1} (488 nm). The absorbance of each probe bound to cysteine in buffer was found to be approximately 75−85% of that for the probe bound to β-mercaptoethanol or for unreacted probe in buffer alone—extinction coefficients for unreacted probes are listed in the Molecular Probes Catalogue. L7/L12 concentrations were determined colorimetrically using a Coomassie Plus (Pierce Co.) or Bio-Rad (Bio-Rad Co.) assay standardized with gravimetrically quantified L7/L12. All protein concentrations reported here are for dimeric L7/L12. Labeling efficiencies, based on the appropriate absorbances and extinction coefficients of the bound fluorophores and the measured protein concentrations, were routinely in the range

of 95−100% except for the FITC labeled NTF in which the probe/protein ratio was less than 10% to minimize the possibility of fluorescein−fluorescein energy transfer. We note that nonspectroscopic verification of labeling ratios of L7/L12 with fluorescent sulfhydryl probes has been carried out previously using a [^{14}C]iodoacetamide method which corroborated the spectroscopic based determinations (Hamman et al., 1996a).

Size-Exclusion High-Performance Liquid Chromatography (SE-HPLC). Proteins were purified with a silica-based Toso-Haas, G2000SW, 30 cm × 7.8 mm (i.d.) column. The size of the silica packing particles and pores were 10 mm and 125 Å, respectively. A Perkin-Elmer pressure pump and a Hewlett-Packard diode array detector and software system were utilized. The protein concentrations loaded on the columns were usually greater than 5 μM. The flow rate was kept constant at 1 mL/min using the TMN buffer, and the wavelength interval scanned was 210−650 nm. Either 2−4 mM DTT or 7−15 mM β-mercaptoethanol was added to eluates prior to storage or fluorescence measurements for stabilization of methionine residues. The full-length, hinge-deleted and C-terminal and N-terminal constructs of L7/L12 eluted at different times; specifically, the hinge-deleted variant exhibited the shortest retention time, followed by the full-length protein, the N-terminal fragment, and finally the C-terminal fragment (Hamman, 1994). Labeling of the proteins did not affect their elution time.

Preparation of 70S Ribosomal Cores Lacking L7/L12, Reconstitution of the L7/L12 Variants with the Cores, and Activity of the Ribosomes. Ribosomes were purified from *E. coli* MRE 600 (from Grain Processing Inc., IN), and L7/L12 was selectively removed by treatment with a solution of ethanol and NH_4Cl as previously described (Tokimatsu et al., 1981). Reconstitution of the ribosomal cores with the L7/L12 variants was accomplished by incubating a 4-fold molar excess of L7/L12 dimers with ribosomal cores at 20 or 37 °C in TMND buffer for several minutes. Free L7/L12 was separated from intact ribosomes by ultracentrifugation through a 10% sucrose cushion at 150000*g* for 6 h at 4 °C in a Ti-65 rotor. Activity of the reconstituted particles in poly(U)-dependent polyphenylalanine synthesis was verified as described previously (Zecherle et al., 1992b; Hamman et al., 1996a).

Fluorescence Methodologies. (A) Steady-State Fluorescence. Emission spectra and steady-state polarizations were obtained using an SLM 8000 spectrofluorometer equipped with calcite prism polarizers. All measurements were done at 20 °C unless otherwise indicated. Polarization measurements on 1-PMA and 1,5-AEDANS labeled samples were done using 351 nm excitation; the 5-AF and FITC labeled samples were excited at 488 nm (excitation bandpasses were 4 nm FWHM). Emission was viewed through Schott cut-on filters which were GG051 for pyrene, KV399 for AEDANS, and OG085 for fluorescein—these filters pass wavelengths greater than 370, 380,and 510 nm, respectively. For polarization measurements of labeled proteins reconstituted into ribosomes, the scattering backgrounds (ribosomal cores without probes) were subtracted. Limiting polarization values (P_0) for each probe under the excitation and emission conditions described above were verified by reacting each probe with excess cysteine and then determining the polarization of 2 μM solutions in 90% glycerol at 0 °C. The values obtained were 0.474 for FITC or 5-AF, 0.371 for 1,5-AEDANS, and 0.178 for 1-PMA.

(B) Time-Resolved Fluorescence. Lifetime and dynamic polarization measurements were accomplished using the multifrequency phase and modulation method on an ISS K2 spectrofluorometer. Excitation of the various samples was achieved using either the 488 nm or the 351 nm line of an argon ion laser (Spectra-Physics Model 2045) for the fluorescein or pyrene/AEDANS probes, respectively. The respective emissions were observed through the same filters utilized for the steady-state polarization measurements. For lifetime measurements, the exciting light was polarized parallel to the vertical laboratory axis while the emission was viewed through a polarizer oriented at 55° (Spencer & Weber, 1970). In the multifrequency phase and modulation technique, the intensity of the exciting light is modulated and the phase shift and relative modulation of the emitted light, with respect to the excitation or known lifetime standards, are determined. Phase and modulation lifetimes (τ^P and τ^M) are then calculated according to well-known equations (Spencer & Weber, 1969; Jameson et al., 1984). The measured phase and modulation values may be analyzed as a sum of exponentials by using a nonlinear least-squares procedure wherein the goodness of the fit to a particular model (for example, single or multiple exponentials) is judged by the value of the reduced chi-square (χ^2) (Jameson et al., 1984). Analyses were performed using a constant, frequency-independent standard deviation of 0.2° for phase and 0.004 for modulation.

In addition to fluorescence lifetime determinations, the multifrequency phase and modulation method permits characterization of the rotational modes of fluorophores. In the time domain such information is obtained from anisotropy decay data. The frequency domain equivalent of these data is obtained by differential polarized phase fluorometry, also known as dynamic polarization (Weber, 1977; Gratton et al., 1984; Jameson & Hazlett, 1991; Lim et al., 1995; Brunet et al., 1994). In this approach, the sample is illuminated by parallel polarized light, the intensity of which is modulated at high frequencies. The measured phase delay ($\Delta\Phi$) between the perpendicular and parallel components of the emission can be directly determined as well as the ratio of their ac components, *Y*. For an isotropic rotation one obtains the expressions (Weber, 1977):

$$\Delta\Phi = \tan^{-1}\{(3\omega r_0 6D)/[(k^2+\omega^2)(1+r_0-2r_0^2)+ 6D(6D+2k+kr_0)]\} \quad (1)$$

$$Y^2 = \{[(1-r_0)k+6D]^2+(1-r_0)^2\omega^2\}/\{[(1+2r_0)k+ 6D]^2+(1+2r_0)^2\omega^2\} \quad (2)$$

where r_0 is the limiting anisotropy, *D* the rotational diffusion constant, and *k* the radiative decay constant ($1/\tau$). The dynamic polarization expressions may contain more terms for the case of a fluorophore associated with a macromolecule. In the present case, for example, we wish to distinguish local mobility of the probe from the global rotation of the protein. The precise equations used to model such systems clearly depend upon the complexities of the specific case, such as whether the local motion is anisotropic or hindered and the orientation of the excitation and emission dipoles of the probe with respect to the relevant molecular

Table 1: Polarizations and Lifetimes of Full-Length and Hinge-Deleted L7/L12 Variants and C-Terminal and N-Terminal Fragments[a]

sample	SSP[b]	τ_1 (ns)	f_1	τ_2 (ns)	f_2	χ^2
C-33-F	0.142	4.14	>0.99			1.18
C-33-F[c]	0.192	4.14	>0.99			1.26
C-33-F[d]	0.094	4.16	>0.99			1.25
C-63-F	0.105	4.08	>0.99			0.62
C-89-F	0.191	4.16	1.00			0.72
C-89-F[d]	0.178	4.16	1.00			0.89
C-33-A	0.075	12.9	>0.99			1.00
C-63-A	0.059	12.3	1.00			0.66
C-89-A	0.072	12.0	>0.99			1.55
C-33-P	0.010	154	0.74	5.4	0.26	2.40
C-63-P	0.010	137	0.70	6.4	0.30	1.95
C-89:Δ42−52-F	0.110	3.56	>0.99			0.99
C-89:Δ42−52-F[e]	0.142	3.83	>0.98			0.88
C-89:Δ42−52-A	0.102	13.4	1.00			0.82
NTF-FITC	0.172	3.77	>0.98			1.31
C-89-F CTF	0.152	4.17	>0.99			0.60

[a] Abbreviations: F = fluorescein; A = AEDANS; P = pyrene; SSP = steady-state polarization; f_1 and f_2 are fractional intensities; χ^2 is the reduced chi-square. [b] Polarization values are averages from a minimum of 3 samples; standard deviations are ±0.001. Standard errors associated with the lifetime data are approximately ±0.02 ns (fluorescein), ±0.10 ns (AEDANS), and ±3 ns (pyrene); lifetimes were not affected by homo-FRET transfer. Standard errors associated with the fractional contributions are approximately ±0.02. [c] Exchanged with a 15-fold excess of unlabeled wild-type L7/L12 to abolish intersubunit homo-energy transfer (see following paper: Hamman et al., 1996b). [d] Methionine oxidized monomers. [e] C-89:Δ42−52-F was exchanged with an excess of reduced (unlabeled) C-89:Δ42−52 to abolish intersubunit homo-energy transfer (see Hamman et al., 1996b).

axes in the case of nonspherical proteins (Beechem et al., 1986; Brunet et al., 1994). In the absence of more detailed structural information, we have adopted the simplest, limiting case, i.e.:

$$r(t) = r_0[f_1 \exp(-\tau/\theta_1) + f_2 \exp(-\tau/\theta_2)] \qquad (3)$$

where r_0 is the time zero anisotropy (the limiting anisotropy), τ is the fluorescent lifetime, θ_1 and θ_2 are the rotational correlation times (equal to the Debye rotational relaxation time divided by 3) associated with the "global" and "local" rotations, respectively, and f_1 and f_2 are the fractional changes in anisotropy associated with θ_1 and θ_2, respectively. This equation (3) was converted to the frequency domain by using the method outlined by Weber (1977), and fits were performed using a nonlinear least-squares analysis with software from ISS, Inc. (Champaign, IL). As with the lifetime analysis, frequency-independent standard deviations of 0.2° for phase and 0.004 for modulation were used in the χ^2 routines.

RESULTS

Steady-State Polarization Data. The steady-state polarization data were clearly dependent upon the probe location in the case of both the fluorescein and AEDANS probes, as shown in Table 1. For example, for the fluorescein probes on dimeric proteins, the polarizations were 0.142 (C-33), 0.105 (C-63), and 0.191 (C-89). Similarly, for the AEDANS probe, the polarizations were 0.075 (C-33), 0.059 (C-63), and 0.072 (C-89). The polarization of the AEDANS labeled C-89:Δ42−52 variant was greater than that of the full-length protein, 0.102 compared to 0.072. Steady-state polarization values for fluorescein attached to the C-89 CTF or NTF fragments were 0.152 and 0.172, respectively. The conformational dynamics of the C-terminal and N-terminal domains of L7/L12 associated with the intact ribosome were also investigated. Steady-state polarizations for AEDANS labeled C-63 and C-89 (C-terminal domain) were 0.059 and 0.072, respectively, while for AEDANS labeled C-12 and C-33 (N-terminal domain) polarizations were 0.073 and 0.075, respectively, as shown in Table 2. The polarizations of AEDANS attached to the C-terminal domain did not change significantly compared to the values for free full-length L7/L12, whereas those for AEDANS attached to the N-terminal domain showed a significant increase over free protein (0.073 to 0.167 for C-12 and 0.075 to 0.172 for C-33). Conversely, the polarization of AEDANS attached to the C-terminal domain in the hinge-deletion mutant, C-89:Δ42−52, increased significantly (0.102 to 0.147) upon association with the ribosomal core particle. The fluorescence intensity did not change significantly upon association of any labeled L7/L12 variant with ribosomal cores.

Table 2: Polarizations of AEDANS Labeled L7/L12 Variants Free and Bound to 70S Ribosomal Cores[a]

sample	SSP	SSP
N-terminal domain	(free)	(bound)
C-12	0.073	0.167
C-33	0.075	0.172
C-terminal domain	(free)	(bound)
C-63	0.059	0.062
C-89	0.072	0.079
C-89:Δ42−52	0.102	0.147

[a] Polarization values are averages from a minimum of 3 samples; standard deviations are ±0.001.

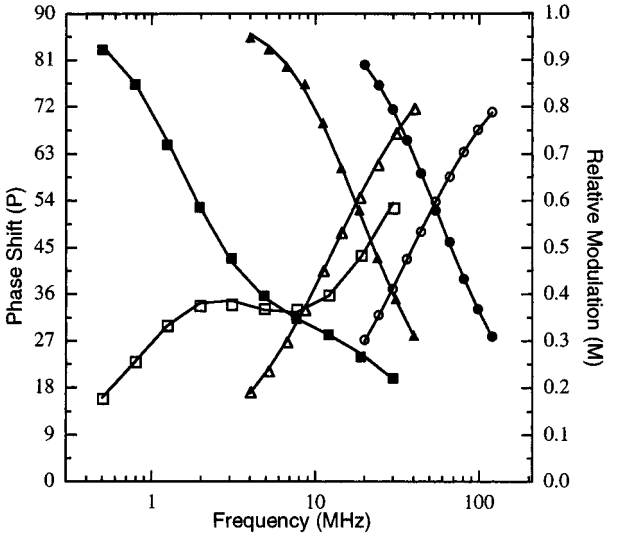

FIGURE 2: Phase (closed symbols) and modulation (open symbols) data for 5-AF (circles), 1,5-AEDANS (triangles), and 1-PMIA (squares) labeled C-33 L7/L12. Solid lines represent the calculated fits to the values given in Table 1.

Time-Resolved Fluorescence. (A) Lifetimes. Representative intensity decay data on the pyrene, AEDANS, and fluorescein probes are shown in Figure 2. The multifrequency phase and modulation data for each full-length probe/protein case was fit to discrete exponential models (no significant improvement in fits was observed utilizing distribution models). In all cases, the data were well-fit, as judged by the reduced chi-square, by single or double

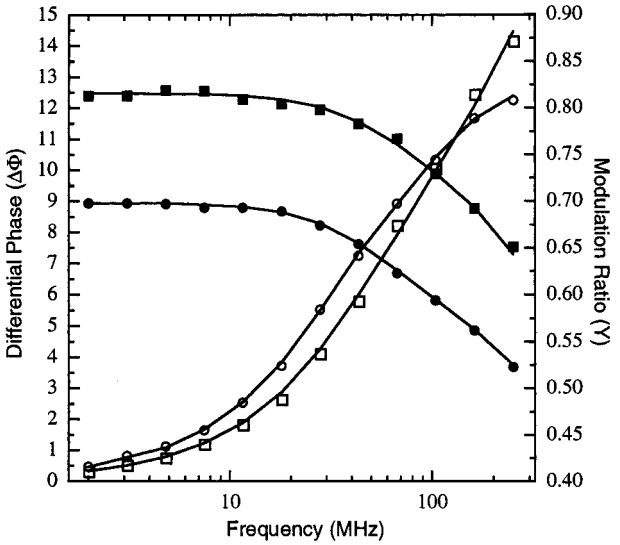

FIGURE 3: Dynamic polarization (phase delay: open symbols; modulation ratio: closed symbols) results on 5-AF labeled C-63 (squares) and C-89 (circles) L7/L12. Solid lines represent the calculated fits to the values given in Table 1.

exponential decays as shown in Table 1. The fluorescein and AEDANS probes were essentially single exponential decays, ranging from 4.08 to 4.16 ns for fluorescein and 12.0 to 12.9 ns for AEDANS, with, in some cases, a very small, short lifetime contribution attributed to scattered light. The data for the pyrene probes, on the other hand, fit best to a double exponential model with, in each case, one component near 150 ns and the other near 6 ns (one notes that the phase data for such widely separated components first increase, then decrease, then increase again as a function of modulation frequency). The lifetimes of the fluorescein probes did not vary significantly with attachment site, and only a small dependence of the lifetime on attachment site was observed for the AEDANS probes. Lifetime and polarization values for fluorescein and AEDANS attached to a hinge-deleted variant are given in Table 1. In these cases, the average lifetimes for the fluorescein derivatives (3.56 and 3.83 ns) were slightly shorter than for the full-length cases (all longer than 4 ns), while the AEDANS lifetime was slightly longer (13.4 ns compared to the full-length range of 12.0−12.9 ns). For fluorescein attached to the C-89 CTF or NTF fragments, the lifetimes were 4.17 and 3.77 ns, respectively.

(B) Dynamic Polarization Data. Dynamic polarization data were obtained on all full-length and hinge-deleted variants as well as the fluorescein labeled NTF and CTF. The data and fits for two representative samples (C-63-F and C-89-F) are shown in Figure 3. In all cases examined, the data fit well to two rotational relaxation times, as judged by the reduced chi-square values (Table 3). The longer values (ρ_1) and the shorter values (ρ_2) shall be referred to as "global" and "local" rotational relaxation times, respectively. In the case of the full-length variants, the "global" rotational relaxation times varied depending on the probe used and the site of attachment. For example, the fluorescein data yielded "global" rotational relaxation times ranging from 15 to 24 ns while the comparable AEDANS values ranged from 16 to 28 ns. The two pyrene cases showed less variation, giving values of 40 and 44 ns. This lifetime-dependent behavior was also evident in the case of the hinge-deleted variants; the fluorescein probe (in the case of singly labeled dimer) gave a "global" rotational relaxation time of 29 ns while a value of 70 ns was observed using the AEDANS probe. "Global" rotational relaxation times near 25 and 14 ns, respectively, were observed for the NTF (labeled with FITC) and C-89 CTF (with 5-AF). The formation of L7/L12 monomers, upon methionine oxidation (see Materials and Methods), led to a significant decrease in the "global" rotational relaxation time as monitored by AF attached to C-33 but not for AF attached to C-89.

Table 3: Dynamic Polarization Parameters for Full-Length and Hinge-Deleted L7/L12 Variants and C-Terminal and N-Terminal Fragments[a]

sample	ρ_1 (ns)	f_1	ρ_2 (ns)	f_2	r_0	χ^2
C-33-F	20.2	0.36	1.82	0.64	0.30[d]	1.15
C-33-F[b]	24.2	0.52	2.10	0.48	0.36	1.20
C-33-F[c]	15.1	0.34	1.28	0.66	0.36	1.95
C-63-F	15.1	0.29	0.95	0.71	0.35	0.60
C-89-F	21.0	0.52	1.45	0.48	0.37	0.90
C-89-F[c]	20.2	0.52	1.40	0.48	0.37	1.08
C-33-A	27.5	0.27	3.02	0.73	0.27	3.12
C-63-A	16.1	0.30	1.96	0.71	0.27	3.20
C-89-A	24.2	0.26	2.72	0.74	0.27	1.71
C-33-P	43.7	0.35	2.77	0.65	0.13	3.44
C-63-P	39.9	0.32	2.22	0.68	0.12	2.97
C-89:Δ42−52-F	18.1	0.36	1.32	0.64	0.28	1.60
C-89:Δ42−52-F[e]	28.8	0.39	1.62	0.61	0.30	0.74
C-89:Δ42−52-A	70.1	0.28	4.10	0.72	0.25	0.92
NTF-F	24.9	0.38	1.48	0.62	0.34	0.91
CTF 89-F	14.2	0.54	0.99	0.46	0.37	1.20

[a] Abbreviations: F = fluorescein; A = AEDANS; P = pyrene; ρ_1 and ρ_2 are rotational relaxation times; f_1 and f_2 are the corresponding fractional contributions to the anisotropy; r_0 is the calculated limiting anisotropy. [b] Exchanged with a 15-fold excess of unlabeled wild-type L7/L12 to abolish intersubunit homo-energy transfer (see Hamman et al., 1996b). Standard errors associated with ρ_1 values are ±0.3 ns (fluorescein), ±0.45 ns (AEDANS), and ±0.6 ns (pyrene). [c] Methionine oxidized monomers. [d] The lower r_0 value here reflects very rapid depolarization due to intersubunit homo-energy transfer (see Hamman et al., 1996b). [e] C-89:Δ42−52-F exchanged with a 15-fold excess of reduced (unlabeled) C-89:Δ42−52 to abolish intersubunit homo-FRET transfer (see Hamman et al., 1996b).

DISCUSSION

A starting point for consideration of the lifetime/polarization data on the various probe/protein systems is the Perrin equation (Weber, 1952):

$$(1/P - 1/3) = (1/P_0 - 1/3)(1 + 3\tau/\rho_h) \qquad (4)$$

where P is the observed steady-state polarization, P_0 is the limiting or intrinsic polarization in the absence of depolarizing influences such as rotation or energy transfer, τ is the excited state lifetime, and ρ_h is the harmonic mean of the Debye rotational relaxation times about the principle axes of rotation. ρ_h is defined as:

$$\rho_h^{-1} = (\rho_1^{-1} + \rho_2^{-1} + \rho_3^{-1})/3 \qquad (5)$$

where ρ_1, ρ_2, and ρ_3 are the rotational relaxation times about the three principle rotation axes. For a spherical molecule, $\rho_1 = \rho_2 = \rho_3 = \rho_0$ and:

$$\rho_0 = 3\eta V/RT \qquad (6)$$

where η is the medium's viscosity, V the molar volume

Table 4: Calculated Rotational Relaxation Times (ns) for 25 kDa Ellipsoids as a Function of Axial Ratio (Modified from Tao, 1969; Steiner & Norris, 1987)[a]

axial ratio	ρ_1	ρ_2	ρ_3	ρ_h
1.0 (s)	33	33	33	33
2.0 (p)	50	43	32	40
2.0 (o)	34	30	22	28
4.0 (p)	113	69	32	66
4.0 (o)	61	63	69	51
10.0 (p)	446	108	33	74
10.0 (o)	143	145	153	147
20.0 (p)	1380	124	33	77
20.0 (o)	284	286	294	288

[a] ρ_1, ρ_2, and ρ_3 are the calculated rotational relaxation times around the three principal rotational axes; ρ_h is the harmonic mean of these three values. Calculated for 20 °C, 0.3 mg/mL hydration, and partial specific volume for L7/L12 of 0.745 mL/g. Abbreviations: (s) spherical, (p) prolate ellipsoid, (o) oblate ellipsoid.

monitored by the probe, R the gas constant, and T the absolute temperature. Using the Perrin equation and the experimentally determined values of P, P_o (see Materials and Methods), and τ, the rotational relaxation times calculated for the full-length dimeric variants range from 2.9 to 7.1 ns for fluorescein and 6.1 to 8.6 ns for AEDANS, while the two pyrene data sets gave calculated rotational relaxation times of 23 and 26 ns. Table 4 shows the rotational relaxation times calculated for a 25 kDa particle for the case of a spherical rotator and for prolate and oblate ellipsoids having different axial ratios. The rotational rates about the three principle axes are given along with their harmonic mean. Clearly, the rotational relaxation times calculated for the various probes attached to L7/L12, using the Perrin equation and the measured steady-state polarizations and lifetimes, are significantly shorter than expected for any of the models considered.

We can thus presume that the probes are monitoring more than one type of motional modality. In the simplest case, one can consider a slow and a fast motion which can be attributed to "global" and "local" motion. The assignment of these terms is somewhat arbitrary. For example, "local" motion was originally attributed to mobility of a probe in excess of that expected by the rotation of a rigid body to which it is attached, due to specific movement of the probe molecule about its point of attachment to the macromolecule (Wahl & Weber, 1967). As techniques improved and as the dynamic nature of proteins became more evident, it was appreciated that "local" motion could include internal or domain motions of the protein as well, such as the segmental flexibility attributed to antibodies (Reidler et al., 1982; Oi et al., 1984; Hanson et al., 1985). The dynamic polarization data in all cases fit well to two rotational relaxation times which varied according to the probe used as well as its location. In the case of the C-33 variants, the "global" relaxation times were 24 ns (fluorescein; singly labeled), 28 ns (AEDANS), and 44 ns (pyrene). This variation suggests that a hierarchy of rotational modalities exists in the labeled L7/L12 molecules and that the probe lifetime effectively determines which range of motion is weighted. In addition to fast "local" motion of the probe around its point of attachment, we interpret the data to indicate that the two C-terminal domains are free to move independently of one another and with respect to the dimeric N-terminal domain. The observation that monomerization of L7/L12 leads to a

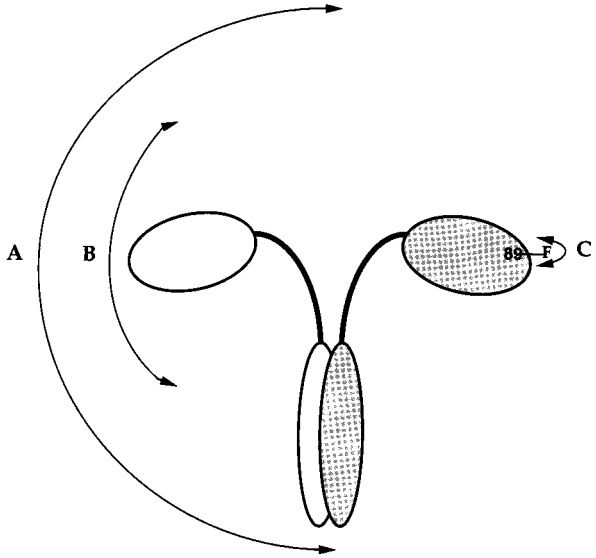

FIGURE 4: Schematic diagram depicting the rotational modalities present in labeled L7/L12: for clarity only one cysteine-linked fluorophore is indicated. (A) Global tumbling of the entire protein. (B) Movement of the C-terminal domains with respect to one another and with respect to the N-terminal domain. (C) Local rotation of the fluorescent probe.

significant reduction in the "global" rotational relaxation time for AF attached to C-33 (from 24 to 15 ns) but not for AF attached to C-89 (21 to 20 ns) also supports this conclusion. In addition, the protein as a whole is rotating. Hence, these rotational modalities are superimposed, but the lifetime of the probe determines which motion is effectively monitored. Fluorescein, with a lifetime near 4 ns, can most effectively monitor the fast "local" motion near its attachment site as well as the movement of the two C-domains relative to the dimeric N-domains, while the longer lifetimes of AEDANS (near 13 ns) and pyrene (average lifetime longer than 100 ns) allow these probes to more effectively monitor the slower overall protein tumbling. These different rotational modalities are depicted in Figure 4. The dynamic polarization data on full-length variants labeled at the C-63 and C-89 positions give similar results, namely, increasing "global" rotational relaxation times with increasing probe lifetime. This consistent difference in observed rotational relaxation times is unlikely to arise from preferential weighting of particular rotational axes over others, as has been observed in some systems (Beechem et al., 1986; Brunet et al., 1994), due to the extensive local motions experienced by the probes.

In the case of the hinge-deleted variants, "global" rotational relaxation times of 29 ns for the singly labeled fluorescein case and 70 ns for the AEDANS case were determined. Interestingly, even though the hinge-deleted variant is 14% smaller in molecular mass than the full-length constructs, the "global" rotational relaxation times monitored with either probe are longer than the corresponding case with the full-length protein. This result suggests that one of the faster depolarizing motions present in the full-length protein is missing or slowed down. Our interpretation is that the motion of the two C-terminal domains, with respect to one another and to the N-terminal domain, is diminished when the hinge region is removed. This conclusion is also supported by energy transfer studies (described in the following paper (Hamman et al., 1996b)) and studies on formation of ground-state tetramethylrhodamine dimers in

specific L7/L12 variants (Hamman et al., 1996a), which indicate that the separation of the C-terminal domains is significantly reduced upon removal of the hinge; i.e., in the hinge-deletion variants the C-terminal domains are drawn much closer together, on average, reducing their motional range. As mentioned in the introduction, several groups have shown that mutants of L7/L12 lacking the hinge region are no longer competent to promote ribosome activity, which could mean that proper function for L7/L12 requires the full extent of mobility between C-terminal and N-terminal domains evident in the full-length proteins but lacking in the hinge-deleted variants.

The slow or "global" rotational relaxation times found for the C- and N-terminal fragments were near 14 and 25 ns, respectively (Table 3). The molecular weights of the monomeric C- and dimeric N-terminal fragments are 7.1 and 10.3 kDa, respectively, and the rotational relaxation times calculated for spherical particles of these masses are 9.1 and 13.4 ns, respectively. The observed value of 25 ns for NTF thus suggests that this domain is nonspherical, in agreement with a recent NMR study (Bocharov et al., 1996). Similarly, the CTF would also appear to be nonspherical, in agreement with X-ray structural studies (Leijonmarck & Liljas, 1987), although not as asymmetric as the NTF.

The time-resolved data presented here thus suggest that L7/L12 possesses considerable flexibility and that the two C-terminal domains and the dimeric N-terminal domain are able to move independently of one another. This conclusion is supported by the fact that the rotational relaxation times observed for the full-length variants, labeled in the C- or N-terminal domains, respectively, are similar to those observed for the purified CTF and NTF constructs, respectively. Previous hydrodynamic studies (see above) have indicated a large axial ratio for L7/L12. These studies, however, were based on bulk transport properties of L7/L12 and hence weigh more heavily those conformations that most contribute to the viscous drag. Based on our fluorescence results, we believe that solutions of L7/L12 contain a mixture of conformational states.

Our steady-state polarization results also directly demonstrated that the independent mobilities of the two C-terminal domains persist when L7/L12 is bound to the ribosome (Table 2), a finding consistent with previous cross-linking studies (Oleinikov et al., 1993a,b). Although these latter studies demonstrated that cross-linking the C-terminal domains of L7/L12 did not impair its ability to support polyphenylalanine synthesis, the independent mobility of the C-terminal domains may be important in other aspects of the normal functioning of the protein.

ACKNOWLEDGMENT

The authors wish to thank Drs. Gregorio Weber, Enrico Gratton, and Michael Helms for valuable discussions.

REFERENCES

Beechem, J. M., Knutson, J. R., & Brand, L. (1986) *Biochem. Soc. Trans. 14*, 832−836.

Bocharov, E. V., Gudkov, A. T., & Arseniev, A. S. (1996) *FEBS Lett. 379*, 291−294.

Brunet, J. E., Vargas, V., Gratton, E., & Jameson, D. M. (1994) *Biophys. J. 66*, 446−453.

Bushuev, V. N., Sepetov, N. F., & Gudkov, A. T. (1984) *FEBS Lett. 178*, 101−104.

Bushuev, V. N., Gudkov, A. T., Liljas, A., & Sepetov, N. F. (1989) *J. Biol. Chem. 264*, 4498−4505.

Caldwell, P., Luk, D., Weissbach, H., & Brot, N. (1978) *Proc. Natl. Acad. Sci. U.S.A. 75*, 5349−5352.

Cowgill, C., Nichols, B., Kenny, J., Butler, P., Bradbury, E., & Traut, R. R. (1984) *J. Biol. Chem. 259*, 15257−15263.

Gratton, E., Jameson, D. M., & Hall, R. D. (1984) *Annu. Rev. Biophys. Bioeng. 13*, 105−124.

Gudkov, A. T., & Behlke, J. (1978) *Eur. J. Biochem. 90*, 309−312.

Gudkov, A. T., Khechinashvili, N., & Bushuev, V. (1978) *Eur. J. Biochem. 90*, 313−318.

Gudkov, A. T., Gongadze, G. M., Bushuev, B. N., & Okon, M. S. (1982) *FEBS Lett. 138*, 229−232.

Gudkov, A. T., Bubunenko, M., & Gryaznova, O. (1991) *Biochimie 73*, 1387−1389.

Gudkov, A. T., Budovskaya, E. V., & Sherstobaeva, N. M. (1995) *FEBS Lett. 367*, 280−282.

Hamel, E., Koka, M., & Nakamoto, T. (1972) *J. Biol. Chem. 247*, 805−814.

Hamman, B. D. (1994) *Conformational Dynamics and Subunit Equilibrium of Escherichia coli Ribosomal Protein L7/L12*, Ph.D. Dissertation, University Microfilms, Ann Arbor, MI.

Hamman, B. D., Oleinikov, A. V., Jokhadze, G. G., Bochkariov, D. E., Traut, R. R., & Jameson, D. M. (1996a) *J. Biol. Chem. 271*, 7568−7573.

Hamman, B. D., Oleinikov, A. V., Jokhadze, G. G., Traut, R. R., & Jameson, D. M. (1996b) *Biochemistry 35*, 16680−16686.

Hanson, D. C., Yguerabide, J., & Schumaker, V. N. (1985) *Mol. Immunol. 22*, 237−244.

Jameson, D. M., & Hazlett, T. L. (1991) in *Biophysical and Biochemical Aspects of Fluorescence Spectroscopy (*Dewey, G., Ed.) pp 105−133, Plenum Press, New York, NY.

Jameson, D. M., Gratton, E., & Hall, R. D. (1984) *Appl. Spectrosc. Rev. 20*, 55−105.

Kirsebom, L. A., Amons, R., & Isaksson, L. A. (1986) *Eur. J. Biochem. 156*, 669−675.

Lee, C. C., Cantor, C., & Wittman-Liebold, B. (1981) *J. Biol. Chem. 259*, 41−48.

Leijonmarck, M., & Liljas, A. (1987) *J. Mol. Biol. 195*, 555−580.

Liljas, A. (1991) *Int. Rev. Cytol. 124*, 105−136.

Luer, C., & Wong, K.-P. (1979) *Biochemistry 18*, 2019−2027.

Luer, C., & Wong, K.-P. (1980) *Biochemistry 19*, 178−183.

Matheson, A. T., Möller, W., Amons, R., & Yaguchi, M. (1980) in *Ribosomes: Structure, Function and Genetics* (Chambliss, G., Ed.) pp 297−332, University Park Press, Baltimore.

Möller, W., & Maassen, J. A. (1986) in *Structure, Function and Genetics of Ribosomes* (Hardesty, B., & Kramer, G., Eds.) pp 309−325, Springer-Verlag Press, New York, NY.

Möller, W., Castleman, H., & Terhorst, C. P. (1970) *FEBS Lett. 8*, 192−196.

Nowotny, P., Ruhl, M., Nowotny, V., May, R. P., Burkhardt, N., Voss, H., & Nierhaus, K. H. (1994) *Biophys. Chem. 53*, 115−122.

Oi, V. T., Vuong, T. M., Hardy, R., Reidler, J., Dangl, J., Herzenberg, L. A., & Stryer, L. (1984) *Nature 307*, 136−140.

Oleinikov, A., Jokhadze, G., & Traut, R. R. (1993a) *Proc. Natl. Acad. Sci. U.S.A. 90*, 9828−9831.

Oleinikov, A., Perroud, B., Wang, B., & Traut, R. R. (1993b) *J. Biol. Chem. 268*, 917−922.

Österberg, R., Sjöberg, B., Liljas, A., & Pettersson, I. (1976) *FEBS Lett. 66*, 48−51.

Reidler, J., Oi, V. T., Carlsen, W., Vuong, T. M., Pecht, I., Herzenberg, L. A., & Stryer, L. (1982*) J. Mol. Biol. 158*, 739−746.

Sommer, A., Etchison, J. R., Gavino, G., Zecherle, G. N., Casiano, C., & Traut, R. R. (1985) *J. Biol. Chem. 260*, 6522−6527.

Spencer, R. D., & Weber, G. (1969) *Ann. N.Y. Acad. Sci. 158*, 361−376.

Spencer, R. D., & Weber, G. (1970) *J. Chem. Phys. 52*, 1654−1660.

Steiner, R. F., & Norris, L. (1987) *Biopolymers 26*, 1189−1204.

Tao, T. (1969) *Biopolymers 8*, 609−632.

Terhorst, C., Wittmann-Liebold, B., & Möller, W. (1972) *Eur. J. Biochem. 88*, 411−419.
Tokimatsu, H., Strycharz, W. A., & Dahlberg, A. E. (1981) *J. Mol. Biol. 152*, 397−412.
Traut, R. R., Tewari, D., Sommer, S., Gavino, G., Olson, H., Perroud, B., & Wang, B. (1986) in *Structure, Function, and Genetics of Ribosomes* (Hardesty, B., & Kramer, B., Eds.) pp 289−309, Springer-Verlag Press, New York, NY.
Traut, R. R., Oleinikov, A. V., Makarov, E., Jokhadze, G. G., Perroud, B., & Wang, B. (1993) in *The Translational Apparatus* (Nierhaus, K. H. , Franceschi, F., Subramanian, A. R., Erdmann, V. A., & Wittmann-Liebold, B., Eds.) pp 521−532, Plenum Press, New York, NY.
Traut, R. R., Debendranath, D., Bochkariov, D., Oleinikov, A. V., Jokhadze, G. G., Hamman, B. D., & Jameson, D. M. (1995) *Biochem. Cell Biol. 73*, 949−958.
Tritton, T. R. (1978) *Biochemistry 17*, 3959−3964.
Tsurugi, K., & Mitsui, K. (1991) *Biochem. Biophys. Res. Commun. 174*, 1318−1323.
Van Agthaven, A. J., Maassen, J. A., Schrier, P. I., & Möller, W. (1975) *Biochem. Biophys. Res. Commun. 64*, 1184−1191.
Wahl, P., & Weber, G. (1967) *J. Mol. Biol. 30*, 371−382.
Weber, G. (1952) *Biochem J. 51*, 145−167.
Weber, G. (1977) *J. Chem. Phys. 66*, 4081−4091.
Weber, G. (1981) *J. Phys. Chem. 85*, 949−952.
Wong, K.-P., & Paradies, H. (1974) *Biochem. Biophys. Res. Commun. 61*, 178−184.
Zecherle, G., Oleinikov, A. V., & Traut, R. R. (1992a) *J. Biol. Chem. 267*, 5889−5896.
Zecherle, G., Oleinikov, A. V., & Traut, R. R. (1992b) *Biochemistry 31*, 9526−9532.

BI9615001